

# Sub-arcsecond Radio Observations of the Dwarf Starburst Galaxy NGC 3077

Daniel Rosa-González<sup>1,2</sup>

<sup>1</sup> *INAOE, Luis Enrique Erro 1. Tonantzintla, Puebla 72840. México.*

<sup>2</sup> *Astrophysics Group, Blackett Laboratory, Prince Consort Road, London SW7 2AZ, United Kingdom.*

Accepted . Received ; in original form 26 June 2018 (Version 006)

## ABSTRACT

We present the first sub-arcsecond radio observations of the nearby dwarf starburst galaxy NGC 3077 obtained with the MERLIN interferometer. We have detected two resolved sources which are coincident with the positions of two discrete X-ray sources detected by Chandra. One of the radio sources is associated with a supernova remnant and the observed radio flux is consistent with having a non-thermal origin. The age of the SNRs of about 760 years is between the average age of the SNRs detected in M82 and those detected in the Milky Way and the Large Magellanic Cloud. We use this detection to calculate a star formation rate (SFR) of  $0.28 \text{ M}_{\odot} \text{ year}^{-1}$  which is similar to the SFR calculated by using far infrared and millimeter observations but larger than the SFR given by optical recombination lines corrected for extinction. The other compact radio source detected by MERLIN which is coincident with the position of an X-ray binary, has the properties of an HII region with a flux density of about  $747 \mu\text{Jy}$  which corresponds to an ionizing flux of  $6.8 \times 10^{50} \text{ s}^{-1}$ . A young massive stellar cluster with a mass of  $\sim 2 \times 10^5 \text{ M}_{\odot}$  detected by the *Hubble Space Telescope* could be the responsible for the production of the ionizing flux.

**Key words:** galaxies: individual (NGC 3077) – galaxies: starburst – radio: interferometry

## 1 INTRODUCTION

The study of small starburst galaxies such as NGC 3077 has been favoured recently mainly because of the implications that these objects have in the *standard* model of galaxy evolution (e.g. Baugh, Cole & Frenk 1996). In the hierarchical scenario, smaller systems form first and then become the building blocks of the massive galaxies that are observed in the local universe. These systems which are the most numerous type of galaxies, could be responsible for an important fraction of the reionization of the universe. Moreover, due to the low gravitational potential of those galaxies the interstellar medium might be allowed to escape from the host more easily contributing to the enrichment of the intergalactic medium at early epochs. However the expelling of newly processed matter depends not only on the mass of the host and the power of the burst but also on the distribution of the interstellar medium and the presence of a dark matter halo surrounding the host galaxy (e.g. Silich & Tenorio-Tagle 2001).

Nearby compact starburst galaxies are excellent laboratories in which to study the starburst phenomenon. In fact, compact starburst galaxies have been used to test the validity of different star forming tracers (e.g. Rosa-González,

Terlevich & Terlevich 2002); to study the interaction of the burst with the interstellar medium (e.g. Martin 1998; Silich et al. 2002); and to study the enrichment of the intergalactic medium due to the break out of superbubbles (e.g. Kunth et al. 2002).

It is only in the nearby universe that the physical processes related to the current starburst event can be studied in great detail. The presence of a recent starburst event—triggered by the interaction of NGC 3077 with M 81 and M 82—has been confirmed by several independent tracers. The IUE ultraviolet (UV) spectra revealed the presence of massive stars not older than  $7 \times 10^7$  years (Benacchio & Galletta 1981). The peak of the P $\alpha$  nebula – a tracer of young star formation regions – (Meier, Turner and Beck 2001; Böker et al. 1999, Figure 1) is located between two CO complexes detected by the Owens Valley Radio Observatory (Walter et al. 2002). Walter et al. conducted a comprehensive multiwavelength study of NGC 3077, relating the atomic and molecular gas with the observed HII regions. By combining CO and emission line observations, they concluded that the star formation efficiency – defined as the ratio between the H $\alpha$  luminosity and the total amount of molecular gas – in NGC 3077 is higher than the corresponding value in M 82. They conclude that the recent star for-

mation activity in NGC 3077 and M 82 is probably due to their interaction with M 81.

The extinction corrected H $\alpha$  flux indicates a star formation rate (SFR) of about  $0.05 M_{\odot}\text{yr}^{-1}$ , concentrated in a region of about 150 pc in diameter (Walter et al. 2002). This value is lower than the SFR given by extinction-free tracers of the SFR like the mm continuum or the far infrared (FIR). In fact, the SFR given by observations at 2.6 mm by Meier et al. (2001) gives a SFR of 0.3 in agreement with FIR measurements from Thronson, Wilton & Ksir (1991).

Maps of radio emission can reveal SNRs and HII regions as well as other tracers of the star forming activity within a galaxy, such as recombination emission lines and FIR radiation. They are closely related to the evolution of massive stars also, therefore, to the recent star forming history of the galaxy (e.g. Muxlow et al. 1994). In this paper we present for the first time radio maps of NGC 3077 with sub-arcsecond angular resolution.

For consistency with previous publications of radio observations we assume a distance to NGC 3077 of 3.2 Mpc throughout the paper (e.g. Tammann & Sandage 1968).

## 2 OBSERVATIONS

NGC 3077 was observed in May 2004 using the MERLIN interferometer, including the Lovell telescope at Jodrell Bank. NGC 3077 and the phase reference source I0954+658 were observed during a total time of about 21.5 hours. The flux density scale was calibrated assuming a 7.086 Jy for 3C 286. The observations were made using the wide field mode and an observing frequency of 4.994 GHz in each hand of circular polarization using a bandwidth of 13.5 MHz. Visibilities corrupted by instrumental phase errors, telescope errors, or external interference were flagged and discarded by using the local software provided by Jodrell Bank Observatory. The unaberrated field of view of  $30''$  in radius allows us to cover the main active star forming region revealed by emission line images (see Figure 1). The data were naturally weighted using a cell size of  $0.015''$ . The images were deconvolved using the CLEAN algorithm described by Högbom (1974). The rms noise over source-free areas of the image was  $\sim 60 \mu\text{Jy beam}^{-1}$ . The final MERLIN spatial resolution after restoring the image with a circular Gaussian beam was  $0.14''$ . At the assumed distance of NGC 3077 this angular size corresponds roughly to 2 pc.

## 3 DISCRETE X-RAY SOURCES AND THEIR RADIO COUNTERPARTS

At X-ray wavelengths, a star formation event is characterized by the presence of diffuse emission associated with hot gas but also by the presence of compact objects associated with SNRs and high mass X-ray binaries (e.g. Fabiano 1989). Recent Chandra observations of NGC 3077 (Ott, Martin & Walter 2003) revealed the presence of hot gas within expanding H $\alpha$  bubbles. Ott et al. found that the rate at which the hot gas is deposited into the halo is a few times the SFR measured by Walter et al. (2002). Ott et al. (2003) found 6 discrete X-ray sources close to the centre of

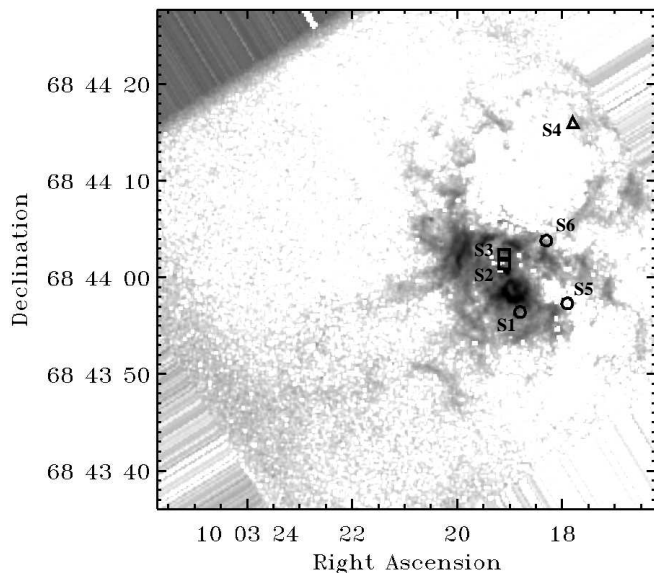


**Figure 1.** P $\alpha$  image of the central part of NGC 3077 showing the regions of recent star formation activity (Böker et al. 1999). The symbols are the discrete sources detected by Chandra. The circles and squares represent possible SNRs and accreting objects, respectively. The triangle indicates the supersoft source characterized in the X-ray by the absence of emission above 0.8 keV. The observed FOV of  $30''$  in radius cover the whole P $\alpha$  emission represented in this figure.

the galaxy, but also associated with bright HII regions (see Figure 1). The details of these are given in Table 1.

The X-ray spectrum of S1, S5 and S6 was found to peak in the range  $\sim 0.8\text{--}1.2$  keV. The X-ray spectral properties suggest that S1, S5 and S6 are SNRs. The X-ray spectra of these sources was best fitted with a Raymond-Smith collisional plasma (Ott et al. 2003). The obtained fluxes and luminosities are given in Table 1. Ott and collaborators derived a radio continuum spectral index of  $\alpha = -0.48$  for S1. However, this determination was based on single dish radio observations with a resolution of  $69''$  (Niklas et al. 1999) and VLA observations with a resolution of  $54''$  (Condon 1987). Recent VLA observations of NGC 3077 at 1.4 GHz have reported an unresolved source located in the same position (Walter et al. 2002).

In Figure 2 we present the resultant MERLIN radio map which shows strong emission coincident, within the Chandra positional errors, with the position of the S1 X-ray source.

The semi-circular morphology of the source showing the presence of bright knots is similar to SNRs observed in other galaxies (e.g. 43.18+58 3 in M 82, Muxlow et al. 1994 or SN1986J in NGC 891, Pérez-Torres, Alberdi & Marcaide 2004). The SNR has a noticeable asymmetry that could be due to interaction with the surrounding media. In fact, a giant molecular cloud (GMC) with a mass of  $\sim 10^7 M_{\odot}$  has been detected in CO (Meier et al. 2001). This GMC has a projected size of  $79 \times 62$  parsecs ( $5.3'' \times 4.1''$ ) and the centroid of the emission is localized just  $1.1''$  from the SNR in the north east direction\*. The interaction of the remnant

\* The position of the GMC is:  $10^{\text{h}}:03^{\text{m}}:18.85^{\text{s}}$ ,  $+68^{\circ}:43':57.8''$

**Table 1.** Discrete X-ray sources detected in NGC 3077. Sources marked with an asterisk have been detected at 5 GHz by the present observations. The proposed type is based only in the X-ray observations. X-ray unabsorbed fluxes and luminosities (columns 6 and 7) are based on the best fitted spectra for each individual source (see text for details).

Source	RA (J2000)	DEC (J2000)	X-Ray Photons (counts)	Proposed Type	Flux ( $\times 10^{-15}$ erg cm $^{-2}$ s $^{-1}$ )	Luminosity ( $\times 10^{37}$ erg s $^{-1}$ )
S1*	10 03 18.8	+68 43 56.4	133 $\pm$ 12	SNR	96.58	14.98
S2	10 03 19.1	+68 44 01.4	114 $\pm$ 11	Accreting	71.56	11.10
S3*	10 03 19.1	+68 44 02.3	119 $\pm$ 11	Accreting	65.14	10.10
S4	10 03 17.8	+68 44 16.0	37 $\pm$ 7	Supersoft Source	5.92	0.92
S5	10 03 17.9	+68 43 57.3	17 $\pm$ 4	SNR	2.06	0.32
S6	10 03 18.3	+68 44 03.8	17 $\pm$ 4	SNR	17.09	2.65

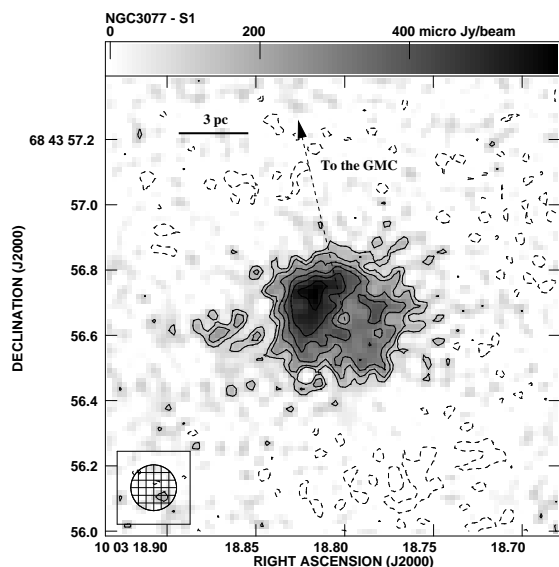


**Figure 2.** MERLIN 5 GHz radio map of the supernova remnant coincident with the X-ray source S1. The obtained rms was 80  $\mu$ Jy beam $^{-1}$ . The contours are at -2, 2, 3, 4.5, 6, 7.5, 9 times the rms. The maximum flux within the image is 595  $\mu$ Jy beam $^{-1}$ . The restoring beam of 0.14'' in diameter is plotted in the bottom right corner of the image. The dashed line points to the position of the GMC described in the text.

with this giant molecular cloud could be the cause of the asymmetry detected in the radio map.

Due to the non-thermal nature of the SNR emission, radio sources with temperatures higher than  $10^4$ K can be unambiguously identified as SNRs. For this radio source we measure a peak flux of  $595 \pm 60 \mu$ Jy/beam which corresponds to a brightness temperature of  $1.24 \pm 0.125 \times 10^4$ K for the given MERLIN spatial resolution at 5 GHz. The angular size of the source – measured on the map using the  $3 \times$  rms contour – is roughly 0.5'' which corresponds to a physical size of about 8 pc at the assumed distance of NGC 3077. If the SNR has expanded with a constant velocity of 5000 km s $^{-1}$  (e.g. Raymond 1984) we deduce that the progenitor star exploded about 760 years ago. This age is longer than the average age of the SNRs detected in M 82 ( $\sim 200$  years) and shorter than the average ages of 2000 and 3000 years of the SNRs detected in the Milky Way and in the LMC respectively (Muxlow et al. 1994).

The assumption of constant expansion velocity is quite

naive, and the size of the observed supernova remnant depends, among others, on the density of the interstellar medium, initial kinetic energy or the size of the cavity created by the stellar wind prior to the supernova explosion. However, there is observational evidence of the existence of cavities created by the stellar winds of the supernova progenitor. In these cavities with densities as low as 0.01 cm $^{-3}$  the velocity of the SNR can reach values of 5000 km s $^{-1}$  (e.g. Tenorio-Tagle et al. 1990, 1991 and references therein). If that is the case of the SNR observed in NGC 3077 the assumed expansion velocity of the supernova blast and the estimated age are reliable. In any case we use the value of 5000 km s $^{-1}$  for the expansion velocity in order to compare our results with those from observations of M 82 (Muxlow et al. 1994).

The life time of massive star progenitors of the SNRs observed in NGC 3077 is much shorter than the Hubble time, therefore the number of observed remnants can be used as a tracer of the current star formation rate. The fact that we observed only one SNR with an estimated age of 760 years can be converted into a supernova rate ( $\nu_{\text{SN}}$ ) of  $1.3 \times 10^{-3}$  year $^{-1}$ . The supernova rate can be translated to the SFR by using,

$$\text{SFR}(M > 5 M_{\odot}) = 24.4 \times \left( \frac{\nu_{\text{SN}}}{\text{year}^{-1}} \right) M_{\odot} \text{year}^{-1} \quad (1)$$

Equation 1 was calculated by using a Scalo IMF, with a lower mass limit of  $5 M_{\odot}$  and an upper limit of  $100 M_{\odot}$  (Condon 1992). In any galaxy most of the stellar mass is located in low mass stars, therefore to calculate the total SFR, including the mass contained in stars with masses lower than  $5 M_{\odot}$  we need to multiply the factor 24.4 in Equation 1 by 9. Combining Equation 1 with the calculated supernova rate we obtain a SFR for NGC 3077 of 0.28  $M_{\odot}$  year $^{-1}$ . The estimated SFR is in reality a upper limit because the presented observations are sensitive to older SNRs which we did not detect. Assuming that the flux of a SNR decay with a rate of  $\sim 1\%$  year $^{-1}$  (e.g. Kronberg & Sramek 1992, Muxlow et al. 1994), the three sigma detection limit of 180  $\mu$ Jy/beam allows to detect older SNRs with ages of 880 years, implying a lower supernova rate  $\nu_{\text{SN}} = 1.14 \times 10^{-3}$  year $^{-1}$ . This fact produce a change in the calculated SFR of about 14%.

The flux density of the SNR was calculated by using the AIPS task IMSTAT which add the observed fluxes within the area defined by the SNR at three times the noise level.

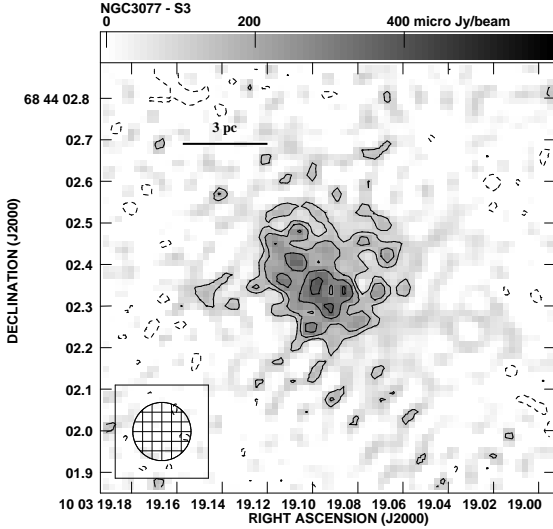


**Figure 3.** MERLIN 5 GHz radio map of the source coincident with the compact X-ray source S3. Contours and restoring beam size as in Figure 3. The maximum flux within the image is  $390 \mu\text{Jy beam}^{-1}$ .

We obtain a flux of  $2100 \pm 175 \mu\text{Jy}$ . For this SNR, the relation between the size and the flux density is consistent with the relation found by Muxlow et al. (1994) for a sample of SNRs detected in M 82 and the LMC. This relation, where the flux density is inversely proportional to the diameter, is not consistent with simple adiabatic losses in a synchrotron-emitting source and an extra source of relativistic particles must come from other reservoir of energy in the form of thermal or kinetic energy present in the remnant (Miley 1980).

The ratio between radio and X-ray fluxes  $R_{r-x} = 5 \times 10^9 F_{5\text{GHz}}/F_x$  is highly variable and depends on the nature of the object, the surrounding media prior to the supernova explosion and the time at which the supernova remnant is observed. Table 2 shows the value of  $R_{r-x}$  for a small sample of SNRs which include the brightest SNRs in our galaxy, Cassiopeia A and Crab nebula. For the galactic SNRs the radio data which includes morphological type, flux and spectral index, was obtained from the Green catalogue (Green 2004). This catalogue is based on observations at 1 GHz. We used the given spectral index to estimate the flux at 5 GHz in order to compare with our observations. For the case of SN1988Z we used the data compiled by Aretxaga et al. (1999) and for the case of NGC7793-S26, the data from Pannuti et al. (2002). The X-ray data are from the compilation by Seward et al. (2005) except S1 and S3 from Ott et al. (2003), SN1006AD from Dyer et al. (2001), SN1988Z from Aretxaga et al. (1999) and NGC7793-S26 from Pannuti et al. (2002). The value of  $R_{r-x}$  goes from  $0.02 \times 10^{-4}$  for the case of SN1006AD to 0.2722 for Vela. The value of  $R_{r-x}$  for S1 is within the observed range.

The other candidates to SNRs – S5 and S6 – were not detected by the present observations. The X-ray fluxes of S5 and S6 are 50 and 6 times respectively lower than the X-ray flux of S1 (see Table 1). Assuming that in both cases the ratio between the X-ray and radio fluxes is equal to the ratio observed in S1,  $R_{r-x}(S1) = 10.8 \times 10^{-4}$  then the expected radio flux for S5 and S6 is below the  $3\sigma$  detection limit.

In the Chandra image of NGC 3077, the sources S2 and S3 are separated by  $1''$ . This separation is roughly the FWHM of the point-spread-function. S2 and S3 each have an X-ray spectrum that was fitted to a power law. These objects were proposed to be either X-ray binaries or background active galactic nuclei (Ott et al. 2003). Figure 3 shows the map of the radio source coincident with the position of S3. The measured intensity peak is  $390 \pm 60 \mu\text{Jy beam}^{-1}$  which is equivalent to a brightness temperature of about 8000 K, typical of an HII region.

Notice that these observations did not rule out the possibility that the observed radio source is an old SNR and further observations at longer wavelength with similar angular resolution and sensitivity are necessary. S3 has a  $R_{r-x} = 5.73 \times 10^{-4}$  which is within the range of values observed in SNRs. However the observed ratio  $R_{r-x}$  in well studied SNRs (Table 2) covers at least 5 order of magnitude therefore the  $R_{r-x}$  value can not be used to discriminate between SNRs and other kind of objects.

Due to the calculated brightness temperature and the X-ray spectrum of S3 the probability that the observed radio emission is coming from an HII region is the most plausible. S3 is probably embebed by the HII nebula but the X-ray flux from the binary and the radio flux have not a common origin.

The free-free emission associated to an HII region can be translated to the number of ionizing photons,  $N_{UV}$  by (Condon 1992),

$$N_{UV} \geq 6.3 \times \left( \frac{T_e}{10^4 \text{K}} \right)^{-0.45} \left( \frac{\nu}{\text{GHz}} \right)^{0.1} \left( \frac{L_T}{10^{20} \text{WHz}^{-1}} \right) \quad (2)$$

The flux density estimated for the HII region associated with S3 was  $747 \pm 127 \mu\text{Jy}$ . If we assume that the observed flux has a thermal origin, we can estimate the thermal luminosity,  $L_T$ . We calculated that the number of UV photons coming from the observed region is  $6.77 \pm 1.15 \times 10^{50} \text{s}^{-1}$ . Taking into account that O stars produce between  $2 \times 10^{49} \text{s}^{-1}$  and  $1 \times 10^{50} \text{s}^{-1}$  UV photons (e.g. Mas-Hesse & Kunth 1991) we conclude that only a few massive stars are responsible for the ionization of the observed nebula. A bright stellar cluster (named cluster # 1 by Harris et al. 2004) was detected by the *Hubble Space Telescope* at just  $0.3''$  from the detected HII region. This cluster with a mass between  $59 \times 10^3$  and  $219 \times 10^3 M_\odot$  and an estimated age of 8 Myr could be the source of ionization of the observed HII nebula. We used the SB99 synthesis model (Leitherer et al. 1999) to estimate the evolution of the ionizing photons for the case of a Salpeter IMF and masses varying between 0.1 and  $100 M_\odot$ . Figure 4 shows the results of the SB99 code for a young cluster with masses within the ranges of masses of the #1 cluster. Using the calculated number of ionizing photons from equation 2 we estimate that the HII region has an age between 3.3 and 5.3 Myr which is just 2 times lower than the age obtained by Harris and collaborators based on optical observations.

Notice that the stellar cluster associated with the HII region is the most massive young cluster observed in NGC 3077 and deeper observations are necessary to obtain radio images of the HII regions associated to the other 55 clusters detected in NGC 3077 by the *Hubble Space Telescope*.

One of the most interesting discrete X-ray source in NGC 3077 is S4. This source exhibited no emission above

**Table 2.** Observed properties of a small sample of SNRs. Second column are the type of the galactic SNRs based on radio observations. Types S and F correspond to shell or filled-centre structure respectively and type C if the SNR shows a composite morphology. Third column are the radio spectral index. Radio and X-ray fluxes are given in the fourth and fifth column. The last column shows the ratio between radio and X-ray fluxes as defined in the text.

Name	Type	Spectral Index	Flux at 5 GHz (mJy)	X-ray Flux ( $\times 10^{-15}$ erg s $^{-1}$ cm $^{-2}$ )	$R_{r-x}$ ( $\times 10^{-4}$ )
S1	–	–	2.10e+00	9.66e+01	10.87
Cassiopeia A	S	0.77	7.88e+05	2.06e+07	19.12
Tycho	S	0.61	2.10e+04	1.99e+06	5.27
Kepler	S	0.64	6.78e+03	6.85e+05	4.95
W49B	S	0.48	1.76e+04	9.00e+06	0.98
RCW103	S	0.50	1.25e+04	1.70e+07	0.37
SN1006-AD	S	0.60	7.23e+00	2.00e+05	0.02
SN1181	F	0.10	2.81e+04	2.70e+04	520
Crab	F	0.30	6.42e+05	2.88e+07	11.14
Vela	C	0.60	6.66e+05	8.87e+04	3755
G292.0+1.8	C	0.40	7.88e+03	2.09e+06	1.89
SN1988Z	–	–	5.30e-01	4.00e+01	6.62
NGC7793-S26	–	0.60	1.24e+00	3.90e+01	15.90

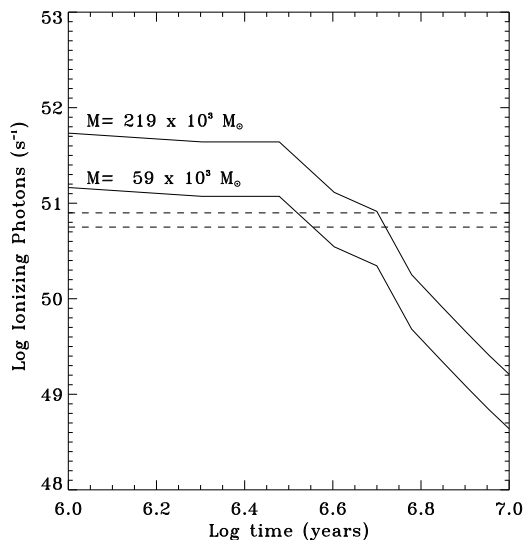


**Figure 4.** Evolution of the production rate of ionizing photons from the SB99 code. The solid lines are the result for two different cluster masses and the dashed horizontal lines are the estimated number of ionizing photons based on the radio observations.

$\sim 0.8$  keV, and was classified as a so-called ‘supersoft source’. The X-ray luminosity of this source is one order of magnitude lower than the luminosities of the sources S1 and S3. This source was fitted by Ott et al. (2003) by using a black body law. Roughly half of the supersoft sources with optical counterparts are yet to be identified with a known type of object (e.g. Di Stefano & Kong 2003). Unfortunately, we did not detect any radio counterpart associated with this source.

#### 4 SUMMARY

The radio observations presented in this paper found 2 of the 6 discrete sources detected in X-ray by the Chandra observatory. These observations resolved for the first time the

SNR detected in radio several decades ago. The compact radio source with a diameter of about  $0.5''$  coincides with a Chandra point source which also shows characteristics typical of a SNR. The SFR of NGC 3077 based on the size of the detected SNR of  $0.28 M_{\odot} \text{yr}^{-1}$  is equal to values derived by continuum mm observations and the SFR given by the FIR both extinction free tracers of the current SFR. The size of the SNR is about 2 times larger than the size of the largest SNR detected in M 82 indicating that the star forming event in NGC 3077 is older than the one in M 82. The other detected source with the characteristics of a compact HII region, coincides with the X-ray source S3, an X-ray binary system. We estimate a flux density of  $747 \mu\text{Jy}$  for this source. Assuming that all this energy has a thermal origin we estimate that only a few massive stars are necessary to ionize the observed nebula. A massive and young stellar cluster observed by the Hubble Space Telescope coincides with the position of both the S3 X-ray source and the HII region.

#### 5 ACKNOWLEDGMENTS

MERLIN is a national facility operated by the University of Manchester at Jodrell Bank Observatory on behalf of PPARC. I gratefully acknowledges the advice and technical support given by Peter Thomasson, Anita Richards and other members of the Jodrell Bank Observatory. I also thank Elena Terlevich, Guillermo Tenorio-Tagle, Roberto Terlevich, Divakara Mayya, Paul O’Neill and Antonio García Barreto for useful discussions. An extensive report from an anonymous referee greatly improved the final version of the paper.

#### REFERENCES

- Aretxaga I., Joguet B., Kunth D., Melnick J., Terlevich R. J., 1999, *ApJ*, 519, L123
- Baugh C. M., Cole S., Frenk C. S., 1996, *MNRAS*, 283, 1361
- Benacchio L., Galletta G., 1981, *ApJL*, 243, 65

- Bi H. G., Arp H., Zimmermann H. U., 1994, *A&A*, 282, 386  
 Böker T., et al., 1999, *ApJS*, 124, 95  
 Condon J. J., 1987, *ApJS*, 65, 485  
 Condon J. J., 1992, *ARAA*, 30, 575  
 Di Stefano R., Kong A.K.H., 2003. *ApJ*, 592, 884  
 Dyer K. K., Reynolds S. P., Borkowski K. J., Allen G. E., Petre R., 2001, *ApJ*, 551, 439  
 Fabbiano, G., 1989, *ARAA*, 27, 87  
 Green D. A., 2004, *BASI*, 32, 335  
 Harris J., Calzetti D., Gallagher J. S., Smith D. A., Conselice C. J., 2004, *ApJ*, 603, 503  
 Högbom J. A., 1974, *A&AS*, 15, 417  
 Jarrett et al., 2002, *The Two Micron All-Sky Survey: Extended Source Images*.  
 Kinney A. L., Bohlin R. C., Calzetti D., Panagia N., Wyse R. F. G., 1993, *ApJS*, 86, 5  
 Kronberg P. P., Sramek R. A., 1992, *xrea.conf*, 247  
 Kunth D., Legrand F., Tenorio-Tagle G., Silich S., Mas-Hesse J. M., Cerviño M., 2002, *Ap&SS*, 281, 261  
 Leitherer C., et al., 1999, *ApJS*, 123, 3  
 Martin C.L., 1998, *ApJ*, 506, 222  
 Mas-Hesse J. M., Kunth D., 1991, *A&AS*, 88, 399  
 McDonald A. R., Muxlow T. W. B., Wills K. A., Pedlar A., Beswick R. J., 2002, *MNRAS*, 334, 912  
 Meier D. S., Turner J. L., Beck S. C., 2001, *Astron. J.*, 122, 1770  
 Miley G., 1980, *ARAA*, 18, 165  
 Moshir et al. 1990, *The IRAS Faint Source Catalog*.  
 Muxlow T.W.B., Pedlar A., Wilkinson P.N., Axon D.J., Sanders E.M., de Bruyn A.G., 1994, *MNRAS*, 266, 455  
 Niklas S., Klein U., Braine J., Wielebinski R., 1995, *A&AS*, 114, 21  
 Ott J., Martin C.L., Walter F., 2003, *ApJ*, 594, 776  
 Ott J., Walter F., Brinks E., 2005, *MNRAS*, 358, 1453  
 Pannuti T. G., Duric N., Lacey C. K., Ferguson A. M. N., Magnor M. A., Mendelowitz C., 2002, *ApJ*, 565, 966  
 Pérez-Torres M.A., Alberdi A., Marcaide J.M., 2004, *7th European VLBI Network*.  
 Prestwich A. H. et al. 2003, *ApJ*, 595, 719  
 Rosa-González D., Terlevich E., Terlevich R., 2002. *MNRAS*, 332, 283  
 Seward F., Slane P., Smith R., and Gaetz T., 2005, *Chandra SN Catalog*<sup>†</sup>  
 Silich S., Tenorio-Tagle G., 2001, *ApJ*, 552, 91  
 Silich S., Tenorio-Tagle G., Muñoz-Tuñón C., Cairos L. M., 2002, *Astron. J.*, 123, 2438  
 Tenorio-Tagle G., Rozyczka M., Franco J., Bodenheimer P., 1991, *MNRAS*, 251, 318  
 Tenorio-Tagle G., Bodenheimer P., Franco J., Rozyczka M., 1990, *MNRAS*, 244, 563  
 Tammann G. A., Sandage A., 1968, *ApJ*, 151, 825  
 Thronson H. A., Wilton C., Ksir A., 1991, *MNRAS*, 252, 543  
 Walter F., Weiss A., Martin C., Scoville N., 2002, *Astron. J.*, 123, 225  
 Walter F., Kerp J., Duric N., Brinks E., Klein U., 1998, *ApJL*, 502, 143

This paper has been produced using the Royal Astronomical Society/Blackwell Science  $\LaTeX$  style file.

<sup>†</sup> available electronically at:  
<http://snrcat.cfa.harvard.edu/index.html>